

A CONVEX MODEL AND L_1 MINIMIZATION FOR MUSICAL NOISE REDUCTION IN BLIND SOURCE SEPARATION*

WENYE MA[†], MENG YU[‡], JACK XIN[§], AND STANLEY OSHER[¶]

To Dave Levermore on his 60th birthday with friendship and appreciation

Abstract. Blind source separation (BSS) methods are useful tools to recover or enhance individual speech sources from their mixtures in a multi-talker environment. A class of efficient BSS methods are based on the mutual exclusion hypothesis of the source signal Fourier spectra on the time-frequency (TF) domain, and subsequent data clustering and classification. Though such methodology is simple, the discontinuous decisions in the TF domain for classification often cause defects in the recovered signals in the time domain. The defects are perceived as unpleasant ringing sounds, the so called musical noise. Post-processing is desired for further quality enhancement. In this paper, an efficient musical noise reduction method is presented based on a convex model of time-domain sparse filters. The sparse filters are intended to cancel out the interference due to major sparse peaks in the mixing coefficients or physically the early arrival and high energy portion of the room impulse responses. This strategy is efficiently carried out by l_1 regularization and the split Bregman method. Evaluations by both synthetic and room recorded speech and music data show that our method outperforms existing musical noise reduction methods in terms of objective and subjective measures. Our method can be used as a post-processing tool for more general and recent versions of TF domain BSS methods as well.

Key words. Blind source separation, time-frequency domain, musical noise, convex model, time-domain sparse filters, l_1 minimization, split Bregman method.

AMS subject classifications. 90C25, 65K10, 68T05.

1. Introduction

Sound signals in daily auditory scenes often appear as mixtures when multiple speakers or sound sources are active. It is of both fundamental and practical interest to recover the sound source signals from the received mixtures with minimal information of the environment, mimicking what human ears can do by paying attention to a selected speaker. Blind source separation (BSS) methods aim to achieve this goal, based on some a-priori knowledge of the source signal properties. Following the physics of sound mixing, let us consider N sources $s_k(t)$, $k=1, \dots, N$, to be convolutively mixed. At M sensors, the recorded mixture signals $x_j(t)$, $j=1, \dots, M$, are :

$$x_j(t) = \sum_{k=1}^N \sum_{d=0}^l h_{jk}(d) s_k(t-d), \quad (1.1)$$

where l is the delay length on the order of 10^3 – 10^4 taps (each tap lasts $1/Fs$ second, Fs is the sampling frequency, e.g. 16000 Hertz) in a standard room, $h_{jk}(d)$ is the discrete

*Received: November 15, 2010; accepted (in revised version): June 18, 2011.

The authors M. Yu and W. Ma contributed equally to this work. M. Yu and J. Xin were partially supported by NSF DMS-0911277 and DMS-0712881; W. Ma and S. Osher were partially supported by NSF DMS-0914561, NIH G54RR021813 and the Department of Defense.

[†]Department of Mathematics, University of California, Los Angeles, CA, 90095, USA (mawenye@math.ucla.edu).

[‡]Department of Mathematics, University of California, Irvine, CA, 92697 USA (myu3@uci.edu).

[§]Department of Mathematics, University of California, Irvine, CA, 92697 USA (jxin@math.uci.edu).

[¶]Department of Mathematics, University of California, Los Angeles, CA, 90095 USA (sjo@math.ucla.edu).

Green's function of the room, also known as the room impulse response (RIR), from source k to receiver j . The (severely ill-posed) mathematical problem is to recover both $h_{jk}(d)$ and $s_k(t)$ from $x_j(t)$.

A major branch of BSS is the so called independent component analysis (ICA) which assumes that the source signals are orthogonal to (or independent of) each other [16]. ICA is a more general methodology than recovering sound signals. The time domain ICA [1, 2] attempts to estimate the h_{jk} 's directly and has to deal with a high dimensional nonconvex optimization problem ([16, 24]). Frequency domain ICA [7, 8, 9] solves an instantaneous ($l=0$) version of (1.1) in each frequency bin after applying the discrete Fourier transform (DFT) to (1.1) frame by frame:

$$X_j(f, \tau) \approx \sum_{k=1}^N H_{jk}(f) S_k(f, \tau), \quad (1.2)$$

where (X_j, H_{jk}, S_k) are the T -point DFT of (x_j, h_{jk}, s_k) respectively, and τ is the frame number. The larger T/l is, the better the approximation. Due to the absence of periodicity in d of h_{jk} and s_k , DFT does not transform convolution to local product exactly. The frequency domain approach is limited to using a long DFT, in addition to computations to sort out scaling and permutation ambiguities when synthesizing multi-frequency estimation of $S_k(f, \tau)$ back to a time domain output [16, 23]. Imperfections and errors in scaling and permutation in the frequency domain may lead to artifacts in the time domain signals at the final output.

The time-frequency (TF) approaches have been developed ([31, 10] among others) more recently. They are based on the working assumption that $S_k(f, \tau)$ and $S_{k'}(f, \tau)$ ($k \neq k'$) are relatively sparse or have almost no overlap in the (f, τ) domain. The non-overlap assumption is satisfied quite well by clean speech signals, though is found to deteriorate in reverberant room (a regular room with reflecting surfaces) conditions [13]. It follows from (1.2) and the non-overlap assumption that

$$X_j(f, \tau) \approx H_{jk}(f) S_k(f, \tau), \quad (1.3)$$

where $k \in [1, N]$ is such that S_k is the dominant source at (f, τ) . The source signals can be classified by clustering on TF features. In the two receiver case (similar to two ears), a common feature vector is:

$$\Theta(f, \tau) = \left[\frac{|X_2(f, \tau)|}{|X_1(f, \tau)|}, \frac{1}{2\pi f} \text{angle}(X_2(f, \tau)/X_1(f, \tau)) \right], \quad (1.4)$$

which are the amplitude ratio and normalized phase difference (phase delay) at each point (f, τ) . The angle ranges in $(-\pi, \pi]$. In view of (1.3), $X_2(f, \tau)/X_1(f, \tau) \approx H_{2k}(f)/H_{1k}(f)$, so the feature vector Θ reflects the Fourier transform of RIRs from the dominant source k . The success of the method relies on the formation of clusters in the histogram of the feature vector. The number of clusters is the number of identified source signals; see Figure 1.1 for an illustration of two peaks in the Θ histogram with input data being a mixture of two speech signals. Each TF point (f, t) whose Θ belongs to cluster C_k (by comparing distances from $\Theta(f, \tau)$ to the cluster centroids) is regarded as occupied by the Fourier spectrum of the k -th source signal. One can then define a binary mask (BM) function

$$M_k(f, \tau) = \begin{cases} 1, & \Theta(f, \tau) \in C_k, \\ 0, & \text{otherwise.} \end{cases} \quad (1.5)$$

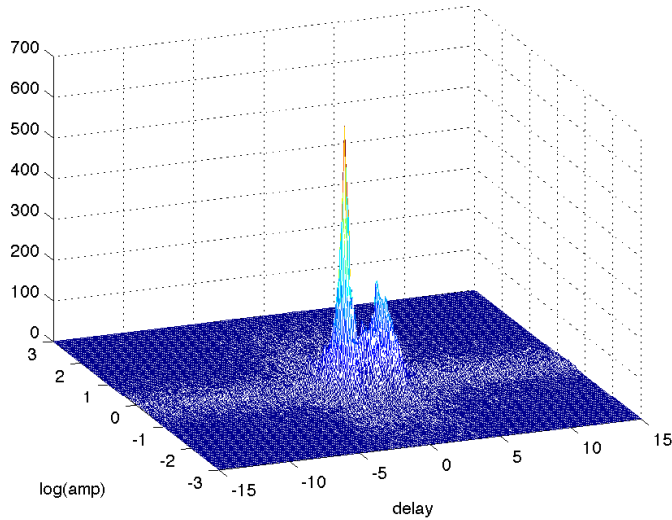


FIG. 1.1. Histogram of Θ feature points (amplitude ratio and phase delay) of 2 mixtures of 2 speech signals, showing 2 distinct peaks.

An estimation of the k -th source in TF domain is

$$\tilde{S}_k(f, \tau) = M_k(f, \tau) X_1(f, \tau), \quad (1.6)$$

where X_1 may be replaced by X_2 as another choice (for multiple sensors, any X_j works for extraction). Finally, taking inverse DFT (iDFT) yields the estimate of $s_k(t)$. The method is robust in the sense that more than two source signals may be recovered from two receivers.

However some remarks are in order. First, the phase of the estimated signal in (1.6) is same as that of the mixture signal. While the amplitude of the dominant k -th source is a good approximation of the mixture signal at those points in C_k , it is not clear that the phase of the k -th signal is close to that of the mixture signal. Phase errors exist in (1.6). Second, the angle function in (1.4) can cause aliasing errors if the phase of $H_{2k}(f)/H_{1k}(f)$ goes out of $(-\pi, \pi]$. For example if $H_{2k}(f)/H_{1k}(f) = \exp\{i\phi_k f\}$, with $|\phi_k f| > \pi$, then the angle part of Θ is equal to the remainder of $\phi_k f$ modulo π , missing the true value $\phi_k f$ and causing artifacts in clustering and classification. Here ϕ_k represents a typical delay of the dominant source in the model (1.1). This restriction translates into an upper limit of a few centimeters on the interdistance of the two receivers, and is recently relaxed [30] by a technique of oversampled Fourier transform and modular arithmetics. Third, the binary mask function M_k makes a zero or one (winner-take-all) decision in the TF domain, which easily leads to nonlinear nonlocal distortions perceived as ringing sounds (musical noise [12]) in the time domain. Fourth, the non-overlap working assumption is violated to various degrees when music signals are in the sources or when the number of source signals increases.

Methods associated with mask based BSS were proposed recently [11, 12] to suppress musical noise. The main ingredients of these methods are: (1) employ-

ing the overlap-add method for reconstructing the waveform outputs from estimated spectra of source signals; (2) using a finer shift of window function while taking short time Fourier transform (STFT); (3) adopting non-binary masks. One choice for (3) is based on the so called sigmoid function, where M_k is defined by $\mathcal{M}_k(f, \tau) = 1/[1 + \exp(g(d_k(f, \tau) - \theta_k))]$, where θ_k and g are shape parameters, and $d_k(f, \tau)$ is the distance between cluster members and their centroids. The other choice for (3) comes from Bayesian inference. The mask function is a conditional probability function $\mathcal{M}_k(f, \tau) = P(C_k | \mathbf{X}(f, \tau))$ where C_k is the k -th cluster and $\mathbf{X}(f, \tau)$ the mixture spectrogram (absolute value of the DFT vector as a function of frequency and frame number). In short, the above noise reduction methods relied on either a gradual change of the Fourier spectra or non-binary masks to increase smoothness of processing in the TF domain.

In this paper, we introduce a simple and efficient *time domain method* to suppress musical noise type artifacts in the output of binary mask based TF domain BSS. Our method can be also used as a postprocessing tool for removing artifacts in any other frequency domain based processing. The idea is to formulate a convex optimization problem for seeking sparse filters to cancel the interference and re-estimate the source signals in the time domain. Our method exploits the spatial difference from sources to receivers and *does not assume the statistics of speech data*. The resulting filter estimation is more economical in data usage and robust for non-stationary speech data [3]. The motivation of incorporating sparsity regularization is to reduce interference by resolving major peaks in the early arrival parts of RIRs, which contain geometric source-receiver information (distances and angles) and are sparsely structured. Sparse filter solutions do not resolve all details of the RIRs, hence avoid overfitting and heavy computational costs. As a result, we effectively reduced errors in phase aliasing and the discontinuous masking operations of the initial TF mask based method. The sparse filters are computed by l_1 norm regularization and the split Bregman method, for which fast convergence was recently studied [22].

The paper is organized as follows. In Section 2, we propose a way to modify the mask function to reduce fuzzy points in the feature space that lie in almost equal distances to two cluster centroids. This treatment reduces clustering errors and extends the TF binary mask based BSS [10] in the regime where the microphone spacing exceeds the effective range of [31] and phase aliasing errors occur. In Section 3, we introduce a convex musical noise suppression model based on a convex optimization problem with l_1 norm regularization. In Section 4, the computational framework by the split Bregman method is shown. In Section 5, evaluations of the proposed method demonstrate its merits in comparison with existing methods. Even in the case of large and unknown microphone spacing, the proposed masking and musical noise reduction method enhances the recovered speech and music signals significantly. The concluding remarks are in Section 6.

2. Initial source estimation

The initial sound separation is carried out by the TF domain binary mask method [31], as described in the introduction, with the K -means algorithm for clustering. We shall however propose some improvements towards the accurate estimation of the feature parameters with less restriction on the receiver interdistances. Because the single source dominance assumption at each TF point may not be valid with the increase of source number N or reverberation time (convolution length D in model (1.1)), we introduce a stricter criterion below for clustering accuracy. At each TF point (f, τ) , the confidence coefficient of $(f, \tau) \in C_k$ is defined by $CC(f, \tau) = \frac{d_k}{\min_{j \neq k} d_j}$,

where d_j is the distance between $\Theta(f, \tau)$ and the centroid of the j -th peak. The new mask function is defined for some $\rho > 0$ as

$$\mathcal{M}_k(f, \tau) = \begin{cases} 1, & (f, \tau) \in C_k \text{ and } CC(f, \tau) \leq \rho, \\ 0, & \text{otherwise.} \end{cases} \quad (2.1)$$

The motivation for the refined mask (2.1) is to reduce the number of fuzzy feature points which have nearly equal distances to at least two cluster centers. The refined mask function (2.1) applies to the situation where the unknown receiver spacing is not small enough and phase aliasing errors are present [31, 10]. Similar to the TF binary mask BSS method of [10], we adopt the amplitude only feature $\Theta(f, \tau) = \left[\frac{|X_1(f, \tau)|}{|X(f, \tau)|}, \dots, \frac{|X_M(f, \tau)|}{|X(f, \tau)|} \right]$, where $|X(f, \tau)|$ is a normalization factor and M is the number of receivers (sensors). Such a phase free feature vector, though robust to receiver inter-distances and free of phase aliasing errors, is found to be less discriminative and produce lower quality separations [10]. Our modified mask function (2.1) helps to compensate for this loss of separation quality, and sets a better stage for the subsequent time-domain noise reduction and quality enhancement of the recovered source signals. Besides the above binary mask based BSS methods, non-binary masks such as sigmoid function based mask and Bayesian inference based mask discussed in Section 1 were also implemented as the initial step of separation for our proposed musical noise reduction method. Further reduction of musical noise is observed for these methods as well after our post-processing.

3. Musical noise reduction model

Let us first consider the determined case of mixing model with 2 sensors and 2 sources ($N = M = 2$). The output signals of the TF domain mask based BSS are denoted as $y_k(t)$, $k = 1, 2$. The mixing model (1.1) can be abbreviated as $x_j(t) = \sum_{k=1}^2 h_{jk} * s_k$, where the star denotes linear convolution (the inner sum of (1.1)). The following algebraic identities hold:

$$\begin{aligned} h_{22} * x_1(t) - h_{12} * x_2(t) &= (h_{22} * h_{11} - h_{12} * h_{21}) * s_1(t), \\ h_{21} * x_1(t) - h_{11} * x_2(t) &= (h_{21} * h_{12} - h_{11} * h_{22}) * s_2(t). \end{aligned} \quad (3.1)$$

The identities are also known in communication theory as cross-channel cancellation for blind channel identification [27]. Now the modeling idea is to replace the convolutions of source signals on the right hand side of (3.1) by the initial separations y_1 and y_2 respectively. We then seek a pair of filters u_{jk} , $j, k = 1, 2$, such that

$$u_{1k} * x_1 - u_{2k} * x_2 \approx y_k. \quad (3.2)$$

In general, y_1 or y_2 may differ from $(h_{22} * h_{11} - h_{12} * h_{21}) * s_1(t)$ or $(h_{21} * h_{12} - h_{11} * h_{22}) * s_2(t)$ by a convolution [24]. Identities (3.1) imply a family of solutions to (3.2) of the form $u_{11} = g_1 * h_{22}$ ($u_{12} = g_2 * h_{21}$) and $u_{21} = g_1 * h_{12}$ ($u_{22} = g_2 * h_{11}$), where g_1 and g_2 are a pair of unknown filters. In other words, the solutions u_{jk} may differ from the room impulse responses (RIRs, or the h_{jk} 's) by a convolution g_k . The optimal choice of g_1 (g_2) is to minimize the length or support of $g_1 * h_{12}$ ($g_2 * h_{11}$) and $g_1 * h_{22}$ ($g_2 * h_{21}$). Without knowledge of RIRs (h_{jk} 's) however, we shall use l_1 norm regularization of u_{1k} and u_{2k} to achieve this goal. The physical reason is to use sparse filters to cancel out the main contributions of interference due to the early arrival parts of the RIRs, which are sparsely structured.

Let us consider a duration D of $y_k(t)$, and seek a pair of sparse filters u_{jk} , $j, k = 1, 2$, to minimize the energy (l_2 norm) of $u_{1k} * x_1 - u_{2k} * x_2 - y_k$ subject to l_1 -norm regularization. The l_2 norm comes from the Gaussian fit of the unknown noise (mismatch) distribution. The resulting convex optimization problem for $t \in D$ is

$$(u_{1k}^*, u_{2k}^*) = \arg \min_{(u_{1k}, u_{2k})} \frac{1}{2} \|u_{1k} * x_1 - u_{2k} * x_2 - y_k\|_2^2 + \mu (\|u_{1k}\|_1 + \|u_{2k}\|_1). \quad (3.3)$$

Let us denote the length of signal in D as L_D and the length of filter solution as L . In matrix form, the convex objective (3.3) becomes

$$u_k^* = \arg \min_{u_k} \frac{1}{2} \|Au_k - y_k\|_2^2 + \mu \|u_k\|_1, \quad (3.4)$$

where u_k is formed by stacking up u_{1k} and u_{2k} , and the $L_D \times 2L$ matrix A is (T is transpose):

$$A = \begin{pmatrix} x_1(1) & x_1(2) & \dots & \dots & x_1(L_D-1) & x_1(L_D) \\ & x_1(1) & \dots & \dots & x_1(L_D-2) & x_1(L_D-1) \\ & & \ddots & & & \vdots \\ -x_2(1) & -x_2(2) & \dots & \dots & -x_2(L_D-1) & -x_2(L_D) \\ & -x_2(1) & \dots & \dots & -x_2(L_D-2) & -x_2(L_D-1) \\ & & \ddots & & & \vdots \\ & & & -x_2(1) & \dots & -x_2(L_D-L+1) \end{pmatrix}^T$$

When u_{1k}^* and u_{2k}^* are found, we compute $u_{1k}^* * x_1 - u_{2k}^* * x_2$ for a better approximation of s_k with musical noise reduced.

The sparsity regularization is also needed to generalize the model to more than two sources. Let us consider the enhancement for 3 sources from 3 mixtures, where each mixture is the sum of sources coming from different propagation channels as

$$\begin{aligned} x_1 &= h_{11} * s_1 + h_{12} * s_2 + h_{13} * s_3, \\ x_2 &= h_{21} * s_1 + h_{22} * s_2 + h_{23} * s_3, \\ x_3 &= h_{31} * s_1 + h_{32} * s_2 + h_{33} * s_3. \end{aligned} \quad (3.5)$$

Suppose that y_3 is the target for denoising. Let u_j , $j=1,2,3$, be the cancellation filters. If the filters satisfy

$$u_1 * h_{11} + u_2 * h_{21} + u_3 * h_{31} = 0, \quad (3.6)$$

$$u_1 * h_{12} + u_2 * h_{22} + u_3 * h_{32} = 0, \quad (3.7)$$

then

$$u_1 * x_1 + u_2 * x_2 + u_3 * x_3 = (u_1 * h_{13} + u_2 * h_{23} + u_3 * h_{33}) * s_3. \quad (3.8)$$

To find u_j , $j=1,2,3$, we take the mixtures x_j , $j=1, 2, 3$, in a duration D as the training data. A natural choice is to estimate the cancellation filters by least squares:

$$(u_1^*, u_2^*, u_3^*) = \arg \min_{u_1, u_2, u_3} \frac{1}{2} \|u_1 * x_1 + u_2 * x_2 + u_3 * x_3 - y_3\|_2^2. \quad (3.9)$$

However, numerical experiments have shown that without further constraints the cancellation filters obtained by least squares (3.9) based on the training data in D

do not work well away from the training data. The problem is overfitting. The solutions might memorize the training data. In other words, it can happen that $(u_1 * h_{11} + u_2 * h_{21} + u_3 * h_{31}) * s_1 + (u_1 * h_{12} + u_2 * h_{22} + u_3 * h_{32}) * s_2 = 0$ in D , while neither $(u_1 * h_{11} + u_2 * h_{21} + u_3 * h_{31})$ nor $(u_1 * h_{12} + u_2 * h_{22} + u_3 * h_{32})$ is equal to 0.

There are a few ways to fix overfitting, such as cross-validation, regularization, or Bayesian priors. The approach we take here is regularization which turns out to be efficient. Using l_1 regularization as illustrated for the 2 sources case, we modify the optimization problem (3.9) to

$$(u_1^*, u_2^*, u_3^*) = \arg \min_{u_1, u_2, u_3} \frac{1}{2} \|u_1 * x_1 + u_2 * x_2 + u_3 * x_3 - y_3\|_2^2 + \mu (\|u_1\|_1 + \|u_2\|_1 + \|u_3\|_1). \tag{3.10}$$

Likewise, for M sensors and M sources, $M \geq 3$, we approximate y_k by a linear combination of the mixtures x_j , $j = 1, 2, \dots, M$. When $t \in D$, for a proper value of $\mu > 0$, we minimize:

$$(u_{jk}^*) = \arg \min_{u_{jk}} \frac{1}{2} \left\| \sum_{j=1}^M u_{jk} * x_j - y_k \right\|_2^2 + \mu \sum_{j=1}^M \|u_{jk}\|_1, \tag{3.11}$$

and estimate s_k by $\hat{s}_k = \sum_{j=1}^M u_{jk}^* * x_j$. Though two sensors are enough for mask based BSS methods, the remaining $M - 2$ sensors are also used here for reducing the musical noise.

4. Minimization by Bregman method

In this section, we adapt the split Bregman method and apply it to the musical noise reduction model (3.4) in reverberant conditions such as in a normal room with acoustic reflections. The split Bregman method was introduced in [22] for solving l_1 , total variation, and related regularized problems. It has been recently shown (see e.g. [17, 20]) that the split Bregman algorithm can also be derived by the augmented Lagrangian method (see e.g. [18]). The connection between split Bregman algorithm and Douglas Rachford splitting was addressed in [19]. The split Bregman method aims to solve the unconstrained problem

$$\min_u J(\Phi u) + H(u), \tag{4.1}$$

where J is convex but not necessarily differentiable, H is convex and differentiable, and Φ is a linear operator. The general split Bregman iteration with initial values $d^0 = 0$, $u^0 = 0$, $b^0 = 0$, is

$$d^{k+1} = \arg \min_d \frac{1}{\lambda} J(d) - \langle b^k, d - d^k \rangle + \frac{1}{2} \|d - \Phi u^k\|_2^2, \tag{4.2}$$

$$u^{k+1} = \arg \min_u \frac{1}{\lambda} H(u) + \langle b^k, \Phi(u - u^k) \rangle + \frac{1}{2} \|d^{k+1} - \Phi u\|_2^2, \tag{4.3}$$

$$b^{k+1} = b^k - (d^{k+1} - \Phi u^{k+1}), \tag{4.4}$$

where λ is a positive constant, and $\langle \cdot, \cdot \rangle$ is the regular inner product.

If J is the l_1 norm, the subproblem (4.2) has explicit solutions. The subproblem (4.3) is also easy to solve since the objective is differentiable. Convergence of the split Bregman method for the case of $J(u) = \mu \|u\|_1$ was analyzed [15], and the result is

THEOREM 4.1. Assume that there exists at least one solution u^* of (4.1). Then we have the following properties for the split Bregman iterations (4.2), (4.3), and (4.4):

$$\lim_{k \rightarrow \infty} \mu \|\Phi u^k\|_1 + H(u^k) = \mu \|\Phi u^*\|_1 + H(u^*).$$

Furthermore,

$$\lim_{k \rightarrow \infty} \|u^k - u^*\|_2 = 0$$

if u^* is the unique solution.

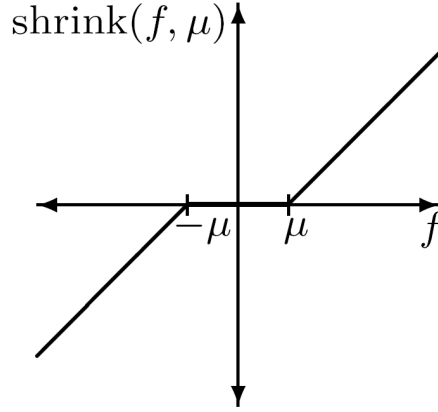


FIG. 4.1. Illustration of the one dimensional shrink operator in the **while** loop of the algorithm in Section 4.

Now we implement the split Bregman method on our proposed musical noise reduction model. Let $J(u) = \mu \|u\|_1$, $\Phi = I$, and $H(u) = \frac{1}{2} \|Au - f\|_2^2$. Setting $d^0 = 0$, $u^0 = 0$, and $b^0 = 0$, we have the iterations:

$$d^{k+1} = \arg \min_d \frac{\mu}{\lambda} \|d\|_1 - \langle b^k, d - d^k \rangle + \frac{1}{2} \|d - u^k\|_2^2, \quad (4.5)$$

$$u^{k+1} = \arg \min_u \frac{1}{2\lambda} \|Au - f\|_2^2 + \langle b^k, u - u^k \rangle + \frac{1}{2} \|d^{k+1} - u\|_2^2, \quad (4.6)$$

$$b^{k+1} = b^k - (d^{k+1} - u^{k+1}). \quad (4.7)$$

Explicitly solving (4.5) and (4.6) gives the simple algorithm

Initialize $u^0 = 0, d^0 = 0, b^0 = 0$
While $\|u^{k+1} - u^k\|_2 / \|u^{k+1}\|_2 > \epsilon$
 (1) $d^{k+1} = \text{shrink}(u^k + b^k, \frac{\mu}{\lambda})$
 (2) $u^{k+1} = (\lambda I + A^T A)^{-1} (A^T f + \lambda(d^{k+1} - b^k))$
 (3) $b^{k+1} = b^k - d^{k+1} + u^{k+1}$
end While

Here shrink is the soft threshold function defined by

$\text{shrink}(v, t) = (\tau_t(v_1), \tau_t(v_2), \dots, \tau_t(v_n))$ for $v = (v_1, v_2, \dots, v_n) \in \mathbb{R}^n$ and $t > 0$, where $\tau_t(x) = \text{sign}(x) \max\{|x| - t, 0\}$; see Figure 4.1 for a one dimensional plot. Noting that the matrix A is fixed, we can precalculate $(\lambda I + A^T A)^{-1}$, so that the iterations only involve matrix multiplication.

Unlike previous applications of Bregman methods to under-determined problems in compressed sensing, here A is an L_D by ML matrix with $L_D \gg ML$ (over-determined). The complexity of calculating $(\lambda I + A^T A)^{-1}$ is $O(L_D(ML)^2) + O((ML)^3) = O(L_D(ML)^2)$. The complexity of each iteration is $O((ML)^2)$. The Forward-Backward splitting method [17] is also a candidate for this problem. It does not involve matrix inversion. But the complexity of each iteration is $O(L_D ML)$. We can accelerate it by precalculating $A^T A$ and $A^T f$ to reduce the complexity in each iteration to $O((ML)^2)$, where $A^T A$ has complexity $O(L_D(ML)^2)$. However, the Forward-Backward splitting method usually needs more iterations to converge than the split Bregman method. We tested various cases and found that the convergence time of the split Bregman method is less than that of the Forward-Backward splitting method by about 40%. Our entire algorithm is summarized as follows:

Input: Observed mixture signals, $x_j, j = 1, \dots, M \geq 2$.

Output: Estimated sources with musical noise suppressed, $\hat{s}_k, k = 1, \dots, N$
($N = M$).

Initial separation: Extract signals $y_k, k = 1, \dots, N$ by TF mask approaches with a proper ρ .

Filter estimation: Apply the **split Bregman** method to obtain the filters $u_{jk}^*, j = 1, \dots, M$ for each source k , according to (3.11).

Musical Noise Suppression: $\hat{s}_k = \sum_{j=1}^M u_{jk}^* * x_j$.

5. Evaluation and comparison

The parameters for the proposed method are chosen as $\mu = \epsilon = 10^{-3}$, $\eta = 1$, $\lambda = 2\mu$, $L_D = 30000$, and $L = 1000$. So matrix A is 30000×2000 , and $A^T A$ is 2000×2000 . As suggested in [12], the STFT frame size is 512 and frame shift is 512/8. For simplicity, we denote by BM1 the so called DUET method of [31], and by BM2 the extended binary mask BSS method of [10], with the modified feature $\Theta(f, \tau)$ in Section 2.

The performance measure [29] is calculated in two steps, provided that the true source signals and sensor noises are known. The first step is to decompose by orthogonal projection an estimate $\hat{s}(t)$ of a source $s(t)$ into a sum of four terms:

$$\hat{s}(t) = s_{target}(t) + e_{interf}(t) + e_{noise}(t) + e_{artif}(t), \quad (5.1)$$

where $s_{target}(t)$ is an allowed deformation of the target source $s(t)$, $e_{interf}(t)$ is an allowed deformation of the interfering (unwanted) sources, $e_{noise}(t)$ for sensor noises, and $e_{artif}(t)$ for artifacts of the separation algorithms such as musical noise or other forbidden distortions of the sources. The second step is to compute performance criteria on the decibel (dB) scale as follows [29, 21]:

- The Signal to Distortion Ratio (SDR)

$$SDR \triangleq 10 \log_{10} \frac{\|s_{target}\|_2^2}{\|e_{interf} + e_{noise} + e_{artif}\|_2^2} \quad (5.2)$$

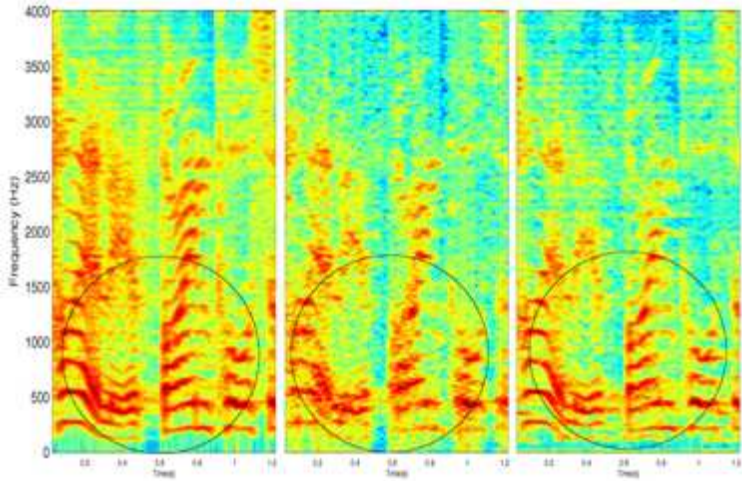


FIG. 5.1. Spectrograms of a source signal (left), the distorted source signal s_d (middle) and the recovered source signal (right). From the left to the middle spectrogram, 80% of the energy is masked out. The reverberation time is 150 ms and the input SIR ≈ -5.9 dB (decibel). Patterns inside the circles illustrate the improvement by the proposed method.

- The Signal to Interferences Ratio (SIR)

$$SIR \triangleq 10 \log_{10} \frac{\|s_{target}\|_2^2}{\|e_{interf}\|_2^2} \quad (5.3)$$

- The Signal to Artifacts Ratio (SAR)

$$SAR \triangleq 10 \log_{10} \frac{\|s_{target} + e_{interf} + e_{noise}\|_2^2}{\|e_{artif}\|_2^2} \quad (5.4)$$

Besides these objective measures, the average Perceptual Evaluation of Speech Quality (PESQ, [26]) score was computed as a measure of performance. This measure was designed to estimate the subjective quality of speech. The output is an estimate of the Mean Opinion Score (MOS), a number between 1 and 5. The meanings of the scores in relation to speech quality are: 1-Bad, 2-Poor, 3-Fair, 4-Good and 5-Excellent.

To test the musical noise reduction portion of our method, synthetic mixture data are used to recover a source signal where energy loss due to binary mask is simulated. The masked signal plays the role of BSS output y_k in Section 3. Measured binaural RIRs (h_{jk} , $j, k = 1, 2$) are used to generate mixtures x_1 and x_2 . For the spectrogram of $h_{11} * s_1$ (or absolute value of $S_{11} = STFT(h_{11} * s_1)$), a mask \mathcal{M} of the same size as S_{11} is defined. The mask is multiplied entry by entry to S_{11} to produce a distorted waveform signal $s_d = iSTFT(S_{11} \circ \mathcal{M})$, where \circ is entrywise product. We recover $h_{11} * s_1$ from the two mixture signals x_1 , x_2 and s_d (in place of y_1) with the Bregman iterations in Section 4. Figure 5 shows the spectrogram of the source signal $h_{11} * s_1$ (left), the spectrogram of the distorted signal s_d (middle) and the spectrogram of the recovered signal (right) in some time frames. The test is repeated under different reverberation times: anechoic, 150 milliseconds (ms), and 580 ms. Though a little interference from s_2 is introduced, i.e. a little decrease of SIR, the gain in SDR [21] is

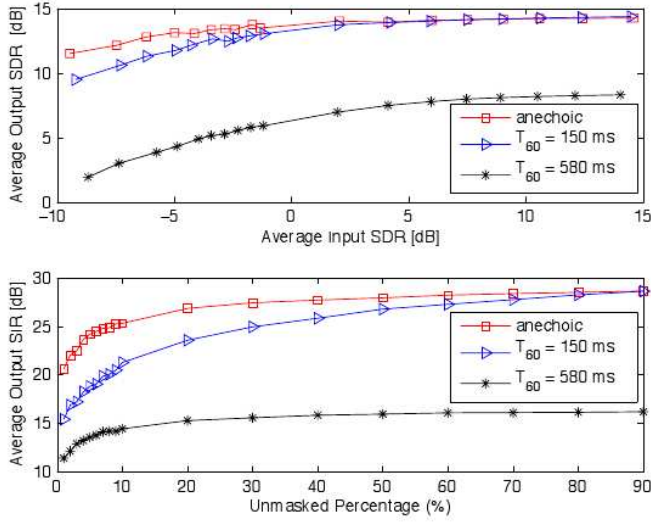


FIG. 5.2. Upper panel: average signal to distortion ratios (SDR) of input and output signals in synthetic test. Lower panel: signal to interference ratio (SIR) vs. unmasked percentage (percentage of 1's) in the mask. The data points in the upper panel have the same unmasked percentage as those in the lower panel.

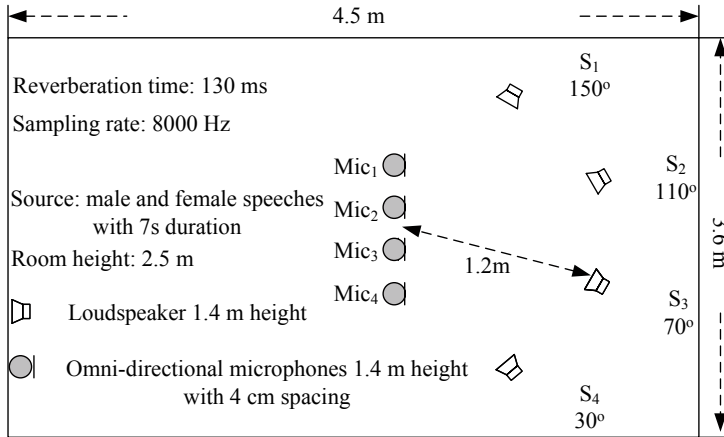


FIG. 5.3. Configuration and parameters of the room recording.

found to be significant in the low input SDR regime; see Figure 5.2. This phenomenon is observed in processing room recorded data as well.

Comparison of several musical noise suppression methods is carried out on room recorded data. The set-up is shown in Figure 5.3. In case of 2 sources, their locations are at S_1 and S_2 in Figure 5.3, and the sensors Mic₁ and Mic₂ provide data for separation and noise suppression. In case of 4 sources, all the loudspeakers and microphones contribute to the musical noise reduction but only Mic₂ and Mic₃ are

Method	PESQ	SIR	SDR	SAR
Input	1.37	0.04	0.02	46.48
BM1 ^[31]	2.24	13.24	6.44	9.37
BM1(0.50)+L1	2.18	9.47	8.58	17.74
BM1(0.25)+L1	2.21	10.07	9.26	17.97
BM1(0.10)+L1	2.22	10.18	9.51	18.94
BM1(0.05)+L1	2.40	13.41	12.18	19.05
SM ^[11]	2.17	11.38	6.52	9.14
SM+L1	2.35	10.34	9.35	17.97
BYM ^[11]	2.33	13.30	7.20	10.20
BYM+L1	2.34	11.25	9.86	18.04

TABLE 5.1. Comparison of musical noise reduction methods on room recorded speech data. Average evaluation results are shown for the 2 sources case. BM1 with conventional mask (1.5); SM (Sigmoid mask); BYM (Bayesian mask). The initial separation for our method (denoted by L1) employs BM1 with refined mask (2.1) (where $\rho=0.50,0.25,0.10,0.05$), SM, and BYM respectively (where $\rho=1$).

Method	PESQ	SIR	SDR	SAR
Input	1.10	-4.49	-4.51	26.54
BM1 ^[31]	1.89	9.39	3.79	6.57
BM1(0.50)+L1	1.90	6.30	5.85	19.06
BM1(0.25)+L1	1.91	6.35	5.89	18.93
BM1(0.10)+L1	1.84	5.63	5.23	18.76
BM1(0.05)+L1	1.75	5.36	4.79	16.86
SM ^[11]	1.71	8.22	2.21	5.40
SM+L1	1.82	4.94	4.31	15.38
BYM ^[11]	1.83	8.21	3.34	6.65
BYM+L1	1.82	4.76	4.36	17.10

TABLE 5.2. Comparison of musical noise reduction methods on room recorded speech data. Average evaluation results are shown for the 4 sources case. BM1 with conventional mask (1.5); SM (Sigmoid mask); BYM (Bayesian mask). The initial separation for our method (denoted by L1) employs BM1 with refined mask (2.1) (where $\rho=0.50,0.25,0.10,0.05$), SM, and BYM respectively (where $\rho=1$).

used for separation. Tables 5.1 and 5.2 list results of different musical noise suppression methods discussed in Section 1. Compared with BM1, sigmoid mask, and Bayesian mask methods, our method leads in the overall quality PESQ [26], and by a significant margin in SDR and SAR. The SIR improvement is however not uniformly better. In the case of 4 sources, SIR improvement lags the other methods. Figure 5.4 illustrates that the refined binary mask method itself cannot achieve higher PESQ than standard BM1 method, and is even significantly worse than BM1 method if ρ is small. Small values of ρ helps the binary mask extract individual source signals with less interference by sacrificing the quality of the target source signal a little. It is highly possible that the perception quality of the refined mask based estimation is

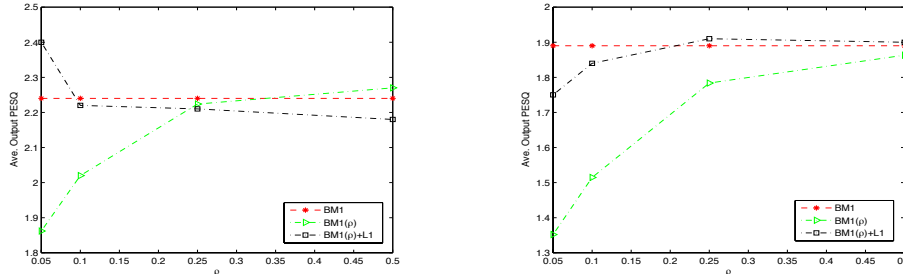


FIG. 5.4. Average output PESQ varies with respect to the mask refined parameter ρ . Left panel and right panel correspond to two-source case and four-source case as Table 5.1 & 5.2 respectively. Red dash line indicates the results by standard BM1 method, which is independent of ρ . Green dash line indicates the results by refined BM1 method at four different values of ρ , while the results by the refined BM1 method with post-processing by the proposed method corresponds to black dash line.

Method	PESQ	SIR	SDR	SAR
Input	1.50	1.90	1.85	33.16
BM2	1.63	16.87	3.58	4.01
SM ^[11]	2.07	22.10	8.86	9.10
BYM ^[11]	2.52	16.54	11.66	14.50
BM2+L1	2.45	16.52	12.81	16.32
SM+L1	2.33	16.66	11.48	17.76
BYM+L1	2.60	15.42	11.73	20.32

TABLE 5.3. Comparison of musical noise reduction methods on speech/music mixtures with unknown large microphone spacing. Refined mask (2.1) with $\rho=0.5$, sigmoid mask and Bayesian mask are employed respectively.

worse than that computed by traditional BM1 method, as shown in Figure 6 for ρ smaller than 0.5. However, these “low interference” estimates y_k , $k=1,2,\dots,N$, provide good input for post-processing in (3.4) and (3.11). This does not mean that the proposed post-processing method always prefers small values of ρ . When the number of sources increases, ρ in the mask (2.1) should increase accordingly to control the growth of zero-paddings. According to our tests, $\rho \in (0.05, 0.1)$ for the two-source case and $\rho \in (0.25, 0.5)$ for four-source case are good settings.

Next we remove Mic₁ and Mic₄ from the set-up of Figure 5.3, so only 2 microphones Mic₂ and Mic₃ are active. The unknown microphone spacing between Mic₂ and Mic₃ is reset to [15, 20] cm, outside the effective range of binary mask BSS methods [31, 10]. The azimuths of the two loudspeakers (emitting speech and music signals sampled at 8000Hz and of 5 second duration) are changed to 0° and 60°. We continue to use the refined mask (2.1) with a nearly optimal value of $\rho=0.5$ based BM2, sigmoid mask, and Bayesian mask respectively as the initial separation for our method. As discussed in Section 2, since BM2 may not work well, eliminating fuzzy feature points by choosing a proper value of ρ helps to gain a good SIR but sacrifices the signal quality. However, as seen in Table 5.3, the overall quality is improved significantly by both the Bayesian mask and our method without losing SIR.

Method	Test Category		>	\approx	<
L1 vs Binary mask	Table 5.1	2 sources	55%	35%	10%
	Table 5.2	4 sources	55%	35%	10%
	Table 5.3	Speech	94%	4%	2%
	Table 5.3	Music	99%	-	1%
L1 vs Sigmoid mask ^[11]	Table 5.1	2 sources	55%	40%	5%
	Table 5.2	4 sources	78%	15%	7%
	Table 5.3	Speech	25%	64%	11%
	Table 5.3	Music	76%	3%	21%
L1 vs Bayesian mask ^[11]	Table 5.1	2 sources	35%	40%	25%
	Table 5.2	4 sources	50%	43%	7%
	Table 5.3	Speech	13%	66%	21%
	Table 5.3	Music	74%	3%	23%

TABLE 5.4. Subjective evaluation on musical noise reduction. Notation $>$ ($<$) means the output of our method is perceived with less (more) musical noise, while \approx means “hard to distinguish”. Binary Mask is BM1 (BM2) for Tables 5.1, 5.2, and 5.3.

Furthermore, we conduct a subjective test on ten listeners with normal hearing to evaluate the reduction of musical noise. The paired comparison test requires each listener to rank the four methods according to the performance of musical noise reduction in the groups of experiments conducted in Tables 5.1, 5.2, and 5.3. The percentage of our method’s preference over three other methods in musical noise reduction is shown in Table 5.4. Since the initially estimated music sources contain more musical noise, the contrasts between these methods on the music channel are more pronounced.

6. Conclusions

In the paper, we propose and evaluate an efficient time domain method for reducing musical noise in the output of TF mask based BSS methods. By a more selective TF mask, we reduce the percentage of fuzzy points on the TF domain to improve separation quality. We employ fast Bregman iterations to minimize a convex l_1 norm regularized objective to compute sparse time-domain filters for musical noise reduction. The time domain filters effectively reduce musical noise and enhance the overall quality of the recovered music and speech signals in terms of both objective and subjective measures.

Acknowledgments. The authors would like to thank Dr. Ernie Esser for many valuable discussions on convex optimization methods, and the anonymous referees for their helpful and constructive comments.

REFERENCES

- [1] S. Amari, S.C. Douglas, A. Chichocki, and H.H. Yang, *Multichannel blind deconvolution and equalization using the natural gradient*, Proc. IEEE Workshop Signal Proc. Adv. Wireless Commun., 101–104, 1997.
- [2] S.C. Douglas and M. Gupta, *Scaled natural gradient algorithms for instantaneous and convolutive blind source separation*, IEEE Int. Conf. Acoust., Speech, Signal Processing, 2, 637–640, 2007.

- [3] Y. Lin, *L1 Norm Sparse Bayesian Learning: Theory and Applications*, Ph.D. Thesis, University of Pennsylvania, 2008.
- [4] H. Buchner, R. Aichner, and W. Kellermann, *TRINICON-based blind system identification with application to multiple-source localization and separation*, Blind Speech Separation, S. Makino, T.W. Lee, and H. Sawada (Eds.), 101–147, 2007.
- [5] T. Yoshioka, T. Nakatani, and M. Miyoshi, *An integrated method for blind separation and dereverberation of convolutive audio mixtures*, Proceedings of the 16th European Signal Processing Conference (EUSIPCO 2008), 2008.
- [6] Y. Huang, J. Benesty, and J. Chen, *A blind channel identification-based two-stage approach to separation and dereverberation of speech signals in a reverberant environment*, IEEE Trans. Speech and Audio Proc., 13(5), 882–895, 2005.
- [7] N. Murata, S. Ikeda, and A. Ziehe, *An approach to blind source separation based on temporal structure of speech signals*, Neurocomp., 41, 1–24, 2001.
- [8] L. Parra and C. Spence, *Convolutive blind separation of non-stationary sources*, IEEE Trans. Speech Audio Processing, 8(3), 320–327, 2000.
- [9] P. Smaragdis, *Blind separation of convolved mixtures in the frequency domain*, Neurocomp., 22(1-3), 21–34, 1998.
- [10] S. Araki, H. Sawada, R. Mukai, and S. Makino, *Underdetermined blind sparse source separation for arbitrarily arranged multiple sensors*, Sig. Proc., 87, 1833–1847, 2007.
- [11] S. Araki, H. Sawada, R. Mukai, and S. Makino, *Blind sparse source separation with spatially smoothed time-frequency masking*, Proc. Int. Workshop on Acoustic Echo and Noise Control, 2006.
- [12] S. Araki, S. Makino, H. Sawada, and R. Mukai, *Reducing musical noise by a fine-shift overlap-add method applied to source separation using a time-frequency mask*, Proc. ICASSP, III, 81–84, 2005.
- [13] S. Araki, H. Sawada, and S. Makino, *K-means based underdetermined blind speech separation*, in Blind Speech Separation, S. Makino, T-W. Lee, H. Sawada (eds), Springer 2007.
- [14] L. Bregman, *The relaxation method of finding the common points of convex sets and its application to the solution of problems in convex programming*, USSR Comput. Math. and Math. Phys., 7, 200–217, 1967.
- [15] J. Cai, S. Osher, and Z. Shen, *Split Bregman methods and frame based image restoration*, Multiscale Model. Simul., 8(2), 337–369, 2009.
- [16] S. Choi, A. Cichocki, H. Park, and S. Lee, *Blind source separation and independent component analysis: A review*, Neural Inform. Process. Lett. Rev., 6, 1–57, 2005.
- [17] E. Esser, *Applications of Lagrangian-based alternating direction methods and connections to split bregman*, CAM report, 09-31, UCLA, 2009.
- [18] R. Glowinski and P. Le Tallec, *Augmented Lagrangian and operator-splitting methods in nonlinear mechanics*, SIAM Stud. Appl. Math., SIAM, 9, 1989.
- [19] S. Setzer, *Split Bregman algorithm, Douglas-Rachford splitting and frame shrinkage*, Scale Space and Variational Methods in Computer Vision, 464–476, 2009.
- [20] X. Tai and C. Wu, *Augmented Lagrangian method, dual methods and split Bregman iteration for ROF model*, Scale Space and Variational Methods in Computer Vision, 502–513, 2009.
- [21] C. Fevotte, R. Gribonval, and E. Vincent, *BSS_EVAL toolbox user guide – Revision 2.0*, Tech. Rep. 1706, IRISA, Rennes, France, April, 2005.
- [22] T. Goldstein and S. Osher, *The split Bregman algorithm for l_1 regularized problems*, SIAM J. Imaging Sci., 2, 323–343, 2009.
- [23] J. Liu, J. Xin, and Y. Qi, *A dynamic algorithm for blind separation of convolutive sound mixtures*, Neurocomp., 72, 521–532, 2008.
- [24] J. Liu, J. Xin, Y. Qi, and F.-G. Zeng, *A time domain algorithm for blind separation of convolutive sound mixtures and l_1 constrained minimization of cross correlations*, Commun. Math. Sci., 7(1), 109–128, 2009.
- [25] S. Osher, M. Burger, D. Goldfarb, J. Xu, and W. Yin, *An iterative regularization method for total variation based image restoration*, SIAM Multiscale Model. and Simu., 4, 460–489, 2005.
- [26] PESQ, *Perceptual evaluation of speech quality (PESQ), an objective method for end-to-end speech quality assessment of narrowband telephone networks and speech codecs*, International Telecommunication Union, Geneva, 862, 2001.
- [27] L. Tong, G. Xu, and T. Kailath, *Blind identification and equalization based on second order statistics: A time domain approach*, IEEE Inform. Theo., 40(2), 340–349, 1994.
- [28] Y. Huang and J. Benesty, *Adaptive multichannel time delay estimation based on blind system identification for acoustic source localization*, Adaptive Signal Processing, Springer, 2003.
- [29] E. Vincent, R. Gribonval, and C. Fvotte, *Performance measurement in blind audio source*

- separation*, IEEE Trans. Audio, Speech, Language Proc., 14(4), 1462–1469, 2006.
- [30] Y. Wang, O. Yilmaz, and Z. Zhou, *A novel phase aliasing correction method for robust blind source separation using DUET*, IEEE Trans. Sig. Proc., to appear.
- [31] O. Yilmaz and S. Rickard, *Blind separation of speech mixtures via time-frequency masking*, IEEE Trans. Sig. Proc., 52(7), 1830–1847, 2004.
- [32] W. Yin, S. Osher, D. Goldfarb, and J. Darbon, *Bregman iterative algorithms for compressed sensing and related problems*, SIAM J. Imag. Sci., 1(1), 143–168, 2008.